processes

MDPI

Article

Application of Residues from Block Freeze-Concentrated Yerba Mate (*Ilex paraguariensis*) Extract as Functional Agents in Smart Biopolymeric Systems Under a Circular Economy Perspective

Ana Caroline Ferreira Carvalho [1,2,*], Julia Prebianca [3], Karine Marafon [1], Amanda Alves Prestes [1], Dayanne Regina Mendes Andrade [4], Cristiane Vieira Helm [5], Jefferson Santos de Gois [6], Paola Tedeschi [7], Carolina Krebs de Souza [2,3] and Elane Schwinden Prudêncio [1,8,*]

1 Postgraduate Program in Food Engineering, Technology Center, Federal University of Santa Catarina, Florianópolis 88040-900, SC, Brazil; karinemarafon@hotmail.com (K.M.); aprestes04@gmail.com (A.A.P.)
2 Department of Chemical Engineering, University of Blumenau, Blumenau 89030-000, SC, Brazil; carolinakrebs@furb.br
3 Postgraduate Program in Chemical Engineering, University of Blumenau, Blumenau 89030-000, SC, Brazil; prebianca@furb.br
4 Postgraduate Program in Food Engineering, Federal University of Parana, Curitiba 82590-300, PR, Brazil; dayannermc@yahoo.com.br
5 Brazilian Agricultural Research Corporation (Embrapa Florestas), Colombo 83411-000, PR, Brazil; cristiane.helm@embrapa.br
6 Department of Analytical Chemistry, Rio de Janeiro State University, Rio de Janeiro 21941-909, RJ, Brazil; jefferson.gois@uerj.br
7 Department of Chemical, Pharmaceutical and Agricultural Sciences, University of Ferrara, 44121 Ferrara, Italy; tdspla@unife.it
8 Department of Food Science and Technology, Federal University of Santa Catarina, Florianópolis 88034-001, SC, Brazil
* Correspondence: anacarolinefc@outlook.com (A.C.F.C.); elane.prudencio@ufsc.br (E.S.P.)

Abstract

Yerba mate (*Ilex paraguariensis*) is a widely consumed beverage recognized for its high antioxidant content and bioactive compounds with health-promoting properties. Concentrating yerba mate extracts represents a valuable opportunity for industrial applications, including food packaging. Block freeze-concentration is a promising technology for concentrating food solutions while preserving functional compounds. In this context, the use of biodegradable polymers combined with natural components derived from by-products aligns with circular economy principles. This study aimed to develop an active and intelligent biopolymer film using residues from the block freeze-concentration of yerba mate extract (ice fraction). The film was produced by the casting method. Block freeze-concentration was performed in three stages, and process efficiency was evaluated using ice fraction 3. The films were characterized for physical, mechanical, thermal, antioxidant (total phenolic content, DPPH, and ABTS), and intelligent properties, including pH-responsive color changes, thickness, biodegradability, barrier performance, molecular structure by FTIR spectroscopy, and morphology by scanning electron microscopy (SEM). The main results showed a total phenolic content of 1.01 ± 0.02 mg GAE g^{-1} of film, 2094 ± 5.00 µmol TE g^{-1} for DPPH, and 1610.00 ± 8.00 µmol TE g^{-1} for ABTS. Color changes observed at different pH levels (4, 7, 10, and 12) demonstrated the film's potential for application in intelligent packaging as a freshness indicator. The film exhibited complete disintegration under soil burial conditions within 45 days. The film presented a water vapor permeability of (1.80 ± 0.01) × 10^{-7} g $H_2O \cdot m^{-1} \cdot s^{-1} \cdot Pa^{-1}$ and an average thickness of 0.26 ± 0.03 mm. As a result, these findings indicate that products derived from

Academic Editor: Dariusz Dziki

Received: 9 March 2026
Revised: 28 March 2026
Accepted: 30 March 2026
Published: 31 March 2026

block freeze-concentration residues of yerba mate extract can be effectively applied in sustainable food packaging systems, contributing to shelf-life extension through antioxidant preservation and intelligent functionality.

Keywords: antioxidant activity; bioactive compounds; biodegradable polymers; pH-sensitive indicators; waste valorization

1. Introduction

The growing concern over the environmental consequences associated with the massive use of petroleum-based conventional plastics has intensified the search for sustainable alternatives in the food packaging sector [1]. These materials, although widely adopted due to their low cost and desirable mechanical performance, exhibit extremely low biodegradability and contribute substantially to global pollution, particularly in terrestrial and aquatic ecosystems [2]. In response, biodegradable, renewable, and environmentally responsible materials have emerged as promising solutions, especially when combined with advanced functionalities that enhance food protection and quality [3,4].

Beyond replacing synthetic polymers with biopolymers, recent technological advances have led to the development of active and intelligent packaging systems, often referred to as smart packaging [5,6]. Active packaging interacts with the food or its surrounding environment by releasing or scavenging compounds that delay spoilage processes, thus extending shelf life and improving microbiological safety [7]. Intelligent packaging, in turn, provides real-time information on food quality by responding to changes in oxidation, pH, or microbial activity [8]. The incorporation of plant extracts rich in bioactive compounds into packaging matrices represents a particularly attractive strategy, enabling the substitution of synthetic additives with natural antioxidants while aligning with consumer demand for clean-label and sustainably sourced ingredients. The antioxidant potential of yerba mate extracts, including their phenolic release behavior in biopolymer films, has already been demonstrated in food packaging systems [9].

Among plant-derived resources, *Ilex paraguariensis*, commonly known as yerba mate, is a rich source of bioactive compounds. Native to South America and deeply embedded in the cultural, economic, and environmental landscapes of Brazil, Argentina, Paraguay, and Uruguay, yerba mate is traditionally consumed as *chimarrão* and *tereré* and is increasingly explored for functional food applications [10]. Its chemical composition is characterized by high levels of phenolic compounds, flavonoids, chlorogenic acids, and alkaloids, which are strongly associated with antioxidant activities widely reported in the literature [11]. These properties make yerba mate a promising candidate for incorporation into packaging systems with active and potentially intelligent functionalities.

The preservation of these bioactive compounds depends strongly on the extraction and concentration technologies employed. Conventional thermal methods may lead to degradation of thermolabile molecules and loss of biological activity [12]. In contrast, block freeze-concentration (BFC) is a non-thermal technology that concentrates liquid extracts through ice crystal formation and separation, preserving heat-sensitive compounds and maintaining functional quality. Studies on freeze-concentrated plant infusions demonstrate that this technique can effectively enhance phenolic content while retaining antioxidant activity [13]. However, BFC inherently generates residual fractions, particularly the dilute phase obtained from melted ice, which may still contain significant amounts of dissolved bioactive compounds [14]. From a sustainability perspective, these residual fractions represent an underexplored opportunity for valorization. Rather than being treated as low-value effluents, they can be redirected as functional ingredients in biodegradable

materials. The incorporation of freeze-concentration residues into biopolymeric matrices enables the transformation of processing by-products into value-added components, contributing antioxidant activity and potentially enabling smart responses within packaging systems. Previous research has shown that yerba mate extracts can be successfully incorporated into biodegradable films, enhancing antioxidant activity and influencing physicochemical properties, supporting the feasibility of using even residual fractions rich in bioactives [15,16].

This strategy aligns closely with the principles of the circular economy, which promotes the maintenance of material value, the reduction in waste generation, and the creation of regenerative production systems [17,18]. Integrating block freeze-concentration processes with the development of biodegradable films reduces effluent production, maximizes resource use, and creates a technological pathway in which waste streams become functional raw materials. Such integration not only improves process sustainability but also contributes to the design of next-generation smart packaging materials based on renewable sources [19].

The objective of this study was to develop biodegradable films incorporating residues obtained from block freeze-concentration of yerba mate extract and to evaluate the influence of this fraction on the structural, functional, and antioxidant properties of the resulting materials. In this context, the study aimed to determine whether these residues can be effectively incorporated into the film matrix and to assess how their presence affects the structural properties and functional performance of the materials. It was hypothesized that the incorporation of these residues could enhance the functional properties of the films, supporting their application as active and sustainable packaging systems. Additionally, the potential of these materials as packaging solutions aligned with circular and bio-based approaches for the food sector was investigated.

2. Materials and Methods

For block freeze concentration, yerba mate (*Ilex paraguariensis*) leaves, ground to 40 mesh, were obtained from the Non-Timber Forest Products Technology Laboratory at Embrapa Florestas (25°17′30″ S latitude and 49°13′27″ W longitude). The film-forming solution was prepared using distilled water, corn starch (viscosity 2000 cps; Milhena, São Paulo, Brazil), glycerol (Neon. São Paulo, Brazil) as plasticizer, and carboxymethylcellulose (CMC, Neon, São Paulo, Brazil) (food-grade off-white powder; viscosity 50–200 cps; Neon, São Paulo, Brazil).

2.1. Block Freeze Concentration Process

The aqueous extract of yerba mate was prepared: 30 g of yerba mate was added to 1 L of distilled water, and the mixture was heated to 100 °C while stirring for 3 min. Subsequently, the extract was cooled to room temperature and then vacuum-filtered to separate the solid residue and obtain the liquid extract (Figure 1A) [20,21].

Gravitational assisted block freeze concentration (BFC) was performed as described by Canella et al. [22] (Figure 1B). First, the yerba mate extract was divided into 200 mL plastic containers and then frozen at -20 ± 2 °C. After the yerba mate aqueous extract was completely frozen, 50% of the initial frozen volume was recovered as the thawed liquid fraction, corresponding to the first concentrate (C1), while the remaining frozen portion constituted the first ice fraction (I1) (Figure 1A). The thawed liquid fraction (C1) was collected and used as the feed solution for the second BFC stage, resulting in a second concentrate (C2) and a second ice fraction (I2) (Figure 1B). Subsequently, the concentrate obtained in the second stage (C2) was used as the feed solution for the third BFC stage, producing a third concentrate (C3) and a third ice fraction (I3) (Figure 1C).

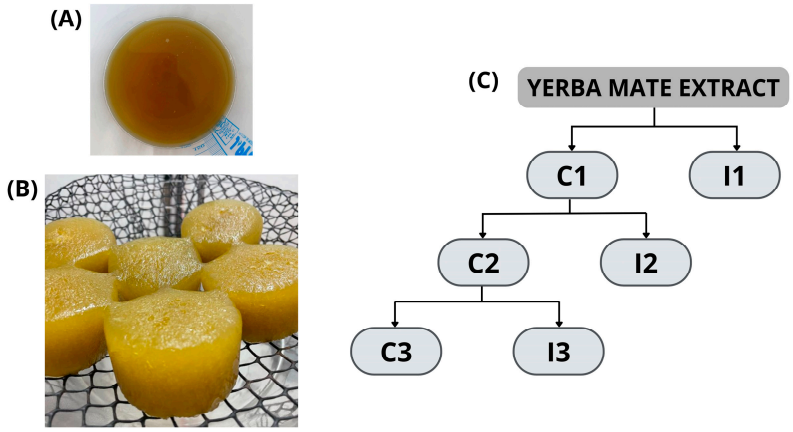

Figure 1. (**A**) Yerba mate extract; (**B**) gravitational assisted block freeze concentration; (**C**) diagram of yerba mate extract freeze concentration. Note: C1, C2, and C3 refer to concentrates of stages 1, 2, and 3, respectively; I1, I2, and I3 refer to ice fractions of stages 1, 2, and 3, respectively.

2.2. Freeze Concentration Parameters

The freeze concentration parameters were evaluated by the concentration factor (CF) according to the calculus of the methodology proposed by Aider and Ounis [23] using Equation (1) with adaptations:

$$Concentration\ Factor = \frac{AG_n}{AG_0}. \quad (1)$$

AG_n is the gallic acid content (mg 100 mL^{-1}) of the concentrated yerba mate extract, and AG_0 is the gallic acid content (mg 100 mL^{-1}) of the initial yerba mate extract.

The process efficiency (PE) was calculated based on the increase in the gallic acid content (AG) in the yerba mate extract (mg 100 mL^{-1}) relative to the AG remaining in the ice (mg 100 mL^{-1}) from each freeze concentration stage, according to Equation (2):

$$Processes\ Efficiency\ (\%) = \frac{AG_C - AG_I}{AG_C} \times 100. \quad (2)$$

AG_c is the gallic acid content (mg 100 mL^{-1}) in the concentrate, and AG_I is the gallic acid content (mg 100 mL^{-1}) in the ice at the end of each freeze concentration stage.

The impurity of the ice was determined based on the gallic acid content (mg 100 mL^{-1}) in the concentrated phase retained in the ice fraction. It was defined as the ratio between the gallic acid concentration in the ice fraction and the gallic acid concentration in the concentrated extract at the end of each cycle. The impurity index for each cycle was calculated according to Equation (3):

$$Impurity\ of\ ice\ (\%) = 100\ (\%) - Processes\ Efficiency\ (\%). \quad (3)$$

2.3. Film Preparation

The film was prepared according to the casting methodology [18]. Initially, 24 g of cornstarch was dispersed in 400 mL of distilled water under continuous stirring. Subsequently, 13.3 g of glycerol, a plasticizer, and 2.4 g of carboxymethylcellulose (CMC) were incorporated into the mixture. The dispersion was heated to 50 °C and maintained under constant agitation for approximately 15 min. The temperature was gradually increased to 80 °C and held for 30 min, promoting complete starch gelatinization and the formation of a homogeneous film-forming solution. Finally, the temperature was raised to 90 °C and maintained for an additional 15 min. After cooling the solution (40 ± 2 °C), 150 mL of the melted ice fraction 3 (I3) was added. The solution was poured into glass containers

(0.08 g cm^{-2}) and placed in a forced-air circulation oven at 45 ± 2 °C for 24 h [5]. The formulation of the biopolymeric films was designed to focus on functionalizing the matrix using the I3 fraction. A blank control (distilled water) was omitted, as the base components (starch, CMC, and glycerol) are widely reported in the literature to have no antioxidant activity or pH-sensitive color properties, thus serving as a known baseline.

2.4. Physical Properties

To evaluate their physical performance, the films were analyzed for thickness, moisture content, water solubility (*WS*), water vapor permeability (*WVP*), and contact angle measurement [4].

Film thickness (5 cm × 5 cm) was measured at five distinct locations on each sample using a digital micrometer (model 02.0005, ZAAS, São Paulo, Brazil) [24]. The moisture content was determined by drying samples of known mass in a hot-air oven (Fanem LTDA, São Paulo, Brazil) at 105 °C until constant weight was achieved [25].

The water solubility (*WS*) of the films was determined using specimens (2 × 2 cm) previously dried and weighed (W_i). The samples were immersed in 30 mL of distilled water under mild agitation for 24 h. After this period, the insoluble fraction was recovered by filtration using pre-dried filter paper (Whatman No. 1, St. Louis, MO, USA). The retained residue was dried in a hot-air oven (MB25, OHAUS, Parsippany, NJ, USA) at 105 °C until constant weight. The final mass (W_f) corresponds to the dry mass of the insoluble film residue, discounting the filter paper mass. Water solubility was calculated as the percentage of solubilized material relative to the initial dry mass, according to Equation (4) [18]:

$$WS = \left(\frac{W_i - W_f}{W_i} \right). \quad (4)$$

The water vapor permeability (*WVP*) of the films was evaluated according to a procedure adapted from Hoffmann et al. [8]. Briefly, 40 g of anhydrous silica gel were placed in a 50 mL centrifuge tube, which was subsequently sealed with the film sample. The assembly was transferred to a desiccator maintained at 25 °C and containing distilled water to provide 100% relative humidity. The tubes were weighed at 30 min intervals over a 4 h period. Mass variation was monitored over time, and the water vapor transmission rate ($\Delta W/\Delta t$) was determined from the slope of the linear regression of mass gain versus time. Water vapor permeability was calculated using Equation (5), where $\Delta W/\Delta t$ corresponds to the slope of the mass variation curve, δ represents the film thickness (m), A is the effective permeation area (m^2), and ΔP denotes the difference in water vapor pressure between the two sides of the film and pure water at 25 °C (Pa):

$$WVP = \left(\frac{\Delta W}{\Delta t} \right) \times \frac{\delta}{A \times \Delta P}. \quad (5)$$

Contact angle analyses were conducted following the methodology described by Jorge et al. [26], with adaptations. Images were acquired using a USB digital microscope at magnifications up to 1000×. Measurements were performed in triplicate, and results were reported as mean ± standard deviation. The contact angle was measured using ImageJ (version 1.x). 10 µL of distilled water was deposited onto the film surface, and images of the liquid–solid interface were captured at 0 s and 180 s for subsequent analysis.

2.5. Mechanical Properties

The mechanical properties of the films were evaluated using a universal testing machine (INSTRON EMIC 23-100, São José dos Pinhais, Brazil) in accordance with ASTM D882 [27]. The maximum force rupture and tensile strength were obtained us-

ing Bluehill Universal software (version 2.x). Film specimens were mounted between two pneumatic grips (EMIC, model GR052, maximum load capacity of 5 kN) and subjected to tensile testing at a constant crosshead speed of 1.0 mm s^{-1}.

The tensile strength (*TS*), elongation at break (*EB*), and Young's Modulus (*E*) were calculated using Equations (6)–(8), respectively [25]:

$$TS\ [MPa] = \frac{F}{\delta \times L}, \quad (6)$$

$$EB\ [\%] = \frac{\Delta L}{L_0} \times 100, \quad (7)$$

$$E\ [MPa] = \frac{\sigma}{\varepsilon}. \quad (8)$$

F is the maximum force at rupture (N), δ is the average thickness (mm), L corresponds to the width of the sample (mm), ΔL is the elongation at break (mm), and L_0 is the initial length of the film sample (mm), σ is the tensile strength/resistance (MPa) and ε is the deformation/elongation at break (mm/mm).

2.6. Structural Properties

The thermal stability of the samples was evaluated by thermogravimetric analysis (TGA). Samples were heated from room temperature to 500 °C at a heating rate of 10 °C min^{-1} under argon at a flow rate of 100 mL min^{-1}. The TGA and DTG curves were obtained and analyzed using Origin 8.5 software [18].

Fourier-transform infrared (FTIR) spectroscopy was performed using a Vertex 70 spectrometer (Billerica, Bruker, Germany) equipped with an attenuated total reflectance accessory. Spectra were recorded in the range of 400–4500 cm^{-1} with a resolution of 4 cm^{-1}, using 16 scans per sample. Spectral data were processed using OPUS software (version 8.x, Bruker) to qualitatively identify functional groups [28].

The microstructure of the films, including surface and cross-section morphology, was examined using a scanning electron microscope (SEM) (VEGA 3, Tescan, Brno, Czech Republic). Prior to analysis, the samples were sputter-coated with a thin layer of gold using a Q150R ES coating system (Quorum Technologies, Lewes, UK). Observations were performed under an accelerating voltage of 10 kV. SEM images of the film surface were acquired at 200×, 500×, and 1000× magnifications, while cross-section images were obtained at 400× magnification [18,25].

2.7. Coloration Parameters

Color attributes and opacity were evaluated using a sphere spectrophotometer (SP60, Lovibond, Amesbury, UK). Opacity was measured in %. The color were expressed in the CIELAB color space, including L^*, which corresponds to brightness, ranging from black (0) to white (100); a^*, which describes the chromatic transition between green (negative values) and red (positive values); and b^*, which represents the variation from blue (negative values) to yellow (positive values) [18].

2.8. Intelligent Freshness Indicator

The prepared films were immersed in solutions at pH 4, 7, 10, and 12 to assess their intelligent response as freshness indicators, as indicated by observable color changes. Colorimetric measurements (L^*, a^*, and b^*) were obtained using a sphere spectrophotometer (SP60, Lovibond). Color differences (ΔE) were determined using Equation (9), in which L_0^*,

a_0*, and b_0* correspond to the initial color parameters of the films prior to exposure to the pH solutions [5]:

$$\Delta E = \left[(L* - L_0*)^2 + (a* - a_0*)^2 + (b* - b_0*)^2\right]^{1/2}. \quad (9)$$

2.9. Biodegradability Test

The film samples were buried in vegetal compost (soil) and maintained under natural environmental conditions. Circular samples with a diameter of 10 cm were used. The biodegradation test was conducted over 45 days, and the results were qualitatively evaluated using photographs [4]. In addition, sample mass loss was monitored throughout the analysis period.

2.10. Total Phenolic Content and Antioxidant Activity

To assess antioxidant activity, total phenolic content, and DPPH and ABTS radical-scavenging activities were analyzed.

The total phenolic content was determined using the Folin–Ciocalteu [29] assay, as described, with gallic acid as the reference standard. A calibration curve was constructed using gallic acid solutions ranging from 1.0 to 9.0 mg $L^{-1,}$ showing good linearity (R^2 = 0.99). Aliquots of the sample extract (0.1–1.0 mL) were transferred to test tubes, followed by the addition of 1.25 mL of Folin–Ciocalteu reagent and 5 mL of sodium carbonate solution (15%, *w*/*v*). After reaction, absorbance was recorded at 720 nm using a UV–Vis spectrophotometer (Shimadzu UV-1800, Kyoto, Japan). Results were expressed as milligrams of gallic acid equivalents per g of film (mg GAE g^{-1}) [30].

The DPPH radical scavenging activity was determined using the method proposed by Brand-Williams et al. [31], which measures the reduction in the stable free radical 2,2-diphenyl-1-picrylhydrazyl (DPPH) in the presence of antioxidant compounds. The decrease in absorbance was monitored at 517 nm. Results were calculated using a Trolox calibration curve and expressed as micromoles of Trolox equivalents per gram of film (μmol TE g^{-1}).

The ABTS radical cation scavenging activity was evaluated according to the method described by Re et al. [32], which relies on antioxidant compounds' ability to donate hydrogen atoms or electrons to neutralize the $ABTS^+$ radical. Absorbance readings were recorded at 734 nm, and antioxidant capacity was quantified using Trolox as the reference standard. Results were expressed as μmol TE g^{-1} of film.

2.11. Statistical Analysis

Statistical analyses were carried out using Statistica software (version 13.5, TIBCO Software Inc., Palo Alto, USA). All experiments were conducted in triplicate, and results are presented as mean values with their respective standard deviations (mean ± standard deviation). Differences among treatments were evaluated by one-way analysis of variance (ANOVA), and when significant effects were observed, Tukey's multiple comparison test was applied. Statistical significance was considered at $p < 0.05$ [33].

3. Results and Discussion

3.1. Freeze Concentration Parameters

During the block freeze concentration process, as the stages advance, the concentration factor increases progressively (1.26 for C1, 2.08 for C2, and 3.05 for C3), directly reflecting the increase in the concentration of gallic acid in the concentrated fraction (Table 1). Moreover, the superior efficiency (69.22 ± 0.20) observed in the third stage, compared with the preceding stages, confirms it as the most efficient phase of the process.

Table 1. Process efficiency and concentration factor of block freeze concentration of yerba mate extract.

Stage	Sample	Gallic Acid (mg L^{-1})	CF	EP (%)	Impurity of the Ice (%)
0	Yerba mate extract	3.84 ^{dB} ± 0.01	-	-	-
1	C1	4.87 ^{c} ± 0.01	1.26 ± 0.01	65.30 ± 0.20	-
	I1	1.69 ^{D} ± 0.01	-	-	34.70 ± 0.01
2	C2	7.99 ^{b} ± 0.01	2.08 ± 0.01	63.95 ± 0.10	-
	I2	2.88 ^{C} ± 0.01	-	-	36.05 ± 0.01
3	C3	11.73 ^{a} ± 0.01	3.05 ± 0.01	69.22 ± 0.20	-
	I3	3.61 ^{A} ± 0.01	-	-	30.78 ± 0.01

Results are expressed as the mean ± standard. $^{a, b, c, d}$ Within a column, different superscript lowercase letters denote significant differences ($p < 0.05$) between the yerba mate extract and C1, C2, and C3. $^{A, B, C, D}$ Within a column, different superscript uppercase letters denote significant differences ($p < 0.05$) between the yerba mate extract and the I1, I2, and I3 fractions.

Similar results were found by Boaventura et al. [13]. In this study, the concentrated fluid showed increasing phenolic compound levels at all freeze-concentration stages (5.33 for C1, 7.60 for C2, and 10.34 for C3). Bredun et al. [34] also carried out a three-stage freeze-concentration process for winemaking by-product (grape pomace extract); the concentration of bioactive compounds increased by 91% for phenolic compounds and 91% for anthocyanins (stage 2). Marafon et al. [35] investigated the performance of acerola pulp (*Malpighia emarginata* DC) during freeze-block concentration, focusing on the behavior of its bioactive compounds. The freeze concentrated fraction obtained in the third stage exhibited the most pronounced concentration effect, with the highest concentration factor among the previous stages (127 for C1, 181 for C2, and 270 for C3).

The third stage (C3) showed the best performance, demonstrating greater concentration capacity of the compounds of interest when compared to the previous stages. This behavior is consistent with the process principle, in which the gradual exclusion of water during successive cycles of freezing and thawing favors the enrichment of the concentrated fraction [36]. The C3 concentrate was selected for preliminary application tests, which indicated promising performance.

The ice fraction generated during the process was evaluated with respect to the full valorization of process streams, in line with the principles of the circular economy [17]. Although traditionally considered a low-value by-product, the ice fraction showed significant retention of bioactive compounds (30.78%) [33]. Given this retention of compounds, it was decided to reuse the ice fraction 3 (I3) to prepare a biodegradable film. This strategy not only reduced waste and effluents from the process but also allowed the incorporation of functional compounds into the film-forming material. The use of melted I3 as a functional ingredient represents an innovative approach that integrates process efficiency, sustainability, and the development of active materials [18,33].

Beyond process efficiency, the selection of the third ice fraction (I3) as a functional ingredient is supported by its relevant retention of bioactive compounds (30.78%). Although ice fractions are typically considered dilute, the progressive increase in solute concentration during successive stages favors the entrapment of phenolic compounds within the ice matrix. As a result, I3 maintained a gallic acid content (3.61 mg L^{-1}) close to that of the initial extract, indicating sufficient bioactive concentration for functional applications.

From a technological perspective, this composition is particularly advantageous, as it provides bioactivity without excessive solute content that could negatively affect film formation or structural integrity. In addition, while the concentrate fraction (C3) is more suitable for direct applications requiring high enrichment, I3 represents a viable alternative for incorporation into biopolymeric systems, where moderate concentrations

are sufficient to promote antioxidant and pH-responsive properties. Therefore, the selection of I3 combines compositional relevance and application feasibility, supporting its use as a functional and sustainable ingredient in developed films.

3.2. Physical Properties

The film had an average thickness of 0.26 ± 0.03 mm, similar to the values reported by Jaramillo et al. [37] (~0.25 mm) and Ceballos et al. [38] (0.25 ± 0.05 mm). These results indicate that the incorporation of the I3 did not alter the thickness, maintaining the uniformity of the polymer matrix and favoring the formation of continuous films.

The film's moisture content was 26.39 ± 0.01%, consistent with values reported for biodegradable films based on starch and plant extracts. Studies such as Leon-Bejarano et al. [39] reported values close to 30%, highlighting the ability of these hydrophilic matrices to retain water due to the presence of polysaccharides and phenolic compounds. This moisture level may promote greater plasticity and resistance to cracking; however, it may also compromise barrier properties and stability, requiring appropriate control of formulation and storage conditions [18].

The water solubility of the developed film was 44.05 ± 3.71%. This behavior can be explained by the higher hygroscopic affinity conferred by hydrophilic compounds present in the I3, which enhances the interaction between the polymer matrix and water. Studies on starch-based films report solubility values ranging from 26.7% to 39.5% [40], indicating that the value obtained in the present study remains within the expected range for hydrophilic polymer systems. This characteristic may represent a limitation for applications involving direct contact with high-moisture or liquid foods, where structural integrity could be compromised. However, the film was specifically designed for use in packaging systems for dry or low-moisture foods, in which exposure to water is minimal. Under these conditions, the observed solubility is not expected to negatively affect its performance [41]. The relatively high solubility should be considered when expanding its application range. Strategies such as crosslinking of the polymer matrix, incorporation of hydrophobic compounds, or the application of surface coatings may be explored to improve water resistance. Therefore, while suitable for dry food applications, further modifications may be required for use in environments with higher water activity [37].

The film showed a water vapor permeability (*WVP*) of (1.80 ± 0.01) × 10^{-7} g $H_2O \cdot m^{-1} \cdot s^{-1} \cdot Pa^{-1}$, indicating a matrix with moderate resistance to water vapor transfer and remaining within the lower range reported for starch-based films (1.0 × 10^{-7} to 4.0 × 10^{-7}) [41]. This result suggests that the presence of hydrophilic compounds from yerba mate did not significantly increase water diffusion, possibly due to structural interactions that promoted a more compact polymer network. Although the *WVP* value is suitable for biodegradable active packaging applications, limitations under high relative humidity conditions should be considered, and formulation adjustments may be recommended to improve barrier efficiency.

The water contact angles of the film confirm a highly wettable surface. At time 0 s, the right angle was 29 ± 1.0°, and the left angle was 33 ± 0.9°; after 180 s, these values dropped to 23.5 ± 0.6° and 23.7 ± 0.4°, respectively (Figure 2). This reduction over time indicates that the drop spread more and/or that water penetrated the polymer matrix, which is typical of films rich in hydroxyl groups (starch/CMC/glycerol), which interact strongly with water through hydrogen bonds. In general, contact angles are used to estimate surface hydrophobicity: higher values indicate greater hydrophobicity, while values <90° indicate hydrophilic materials [42]. In this case, all values were below 90°, reinforcing a hydrophilic profile with high water affinity, consistent with the drop observed between 0 and 180 s.

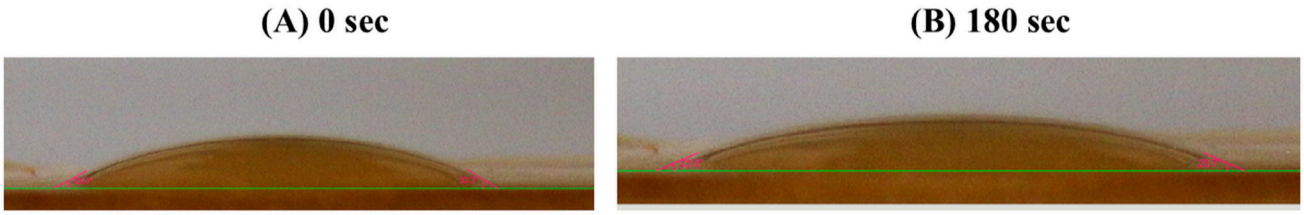

Figure 2. Water contact angle of the film at (**A**) 0 s and (**B**) 180 s, showing the interaction between the film surface and water.

Żołek-Tryznowska et al. [43] reported that starch-based films exhibit water contact angles ranging from 23° to 63°, depending on the starch origin and composition, indicating predominantly hydrophilic surfaces in many cases. For corn starch, the angle was 23.18°. Lopes et al. [44] observed water contact angles ranging from approximately 30.0° to 52.2° in alginate-based edible films, all below 90°, confirming the hydrophilic nature attributed to the polymer's affinity for water.

These results are consistent with the film's high solubility (44.05 ± 3.71%), as more hydrophilic surfaces, characterized by lower contact angles, tend to interact more with water. This greater affinity favors the absorption and diffusion of water in the polymer matrix, facilitating the leaching of soluble components.

Finally, the physical properties of the I3-incorporated films remained consistent with values reported in the literature for pure starch-based films [45], indicating that the residual extract provides functionality without compromising the structural integrity of the matrix.

3.3. Mechanical Properties

The film containing I3 in this study showed a tensile strength of 1.48 ± 0.02 MPa, elongation at break of 60.58 ± 2.21%, and a Young's modulus of 2.13 ± 0.01 MPa, characterizing a flexible material with moderate mechanical resistance. When compared to the results reported by Ceballos et al. [38], who observed higher tensile strength values (2.9–3.2 MPa) and greater elongation (63–80%), the film obtained in the present study exhibited lower mechanical strength, although with similar ductility. This difference may be associated with variations in formulation and processing methods, as well as structural factors such as film thickness, extract distribution, and residual moisture content, which directly influence mechanical performance.

3.4. Structural Properties

The thermogravimetric analysis (TGA) and its corresponding derivative curve (DTG) revealed that the developed film undergoes three distinct stages of mass loss during thermal degradation (Figure 3). In the first stage, between 31 and 238 °C, the film exhibited an approximate 18.0% reduction in mass, mainly due to the evaporation of moisture and low-molecular-weight volatile compounds in the polymer matrix.

The second degradation stage, observed in the temperature range of 238 to 345 °C, was associated with the thermal decomposition of the starch matrix and the plasticizer (glycerol), accounting for approximately 75% of the total mass loss. Finally, the third stage occurred between 345 and 807 °C, during which only a minor mass loss (~12%) was observed, corresponding to the degradation of more thermally stable residues and the formation of char [5]. Carvalho et al. [18] reported a thermal degradation pattern similar to that observed in this study, with mass losses of approximately 17% in the first stage and 70.2% in the second stage, followed by a residual mass of about 8.5%. These values are consistent with the results obtained here, confirming the typical thermal behavior of starch-based films.

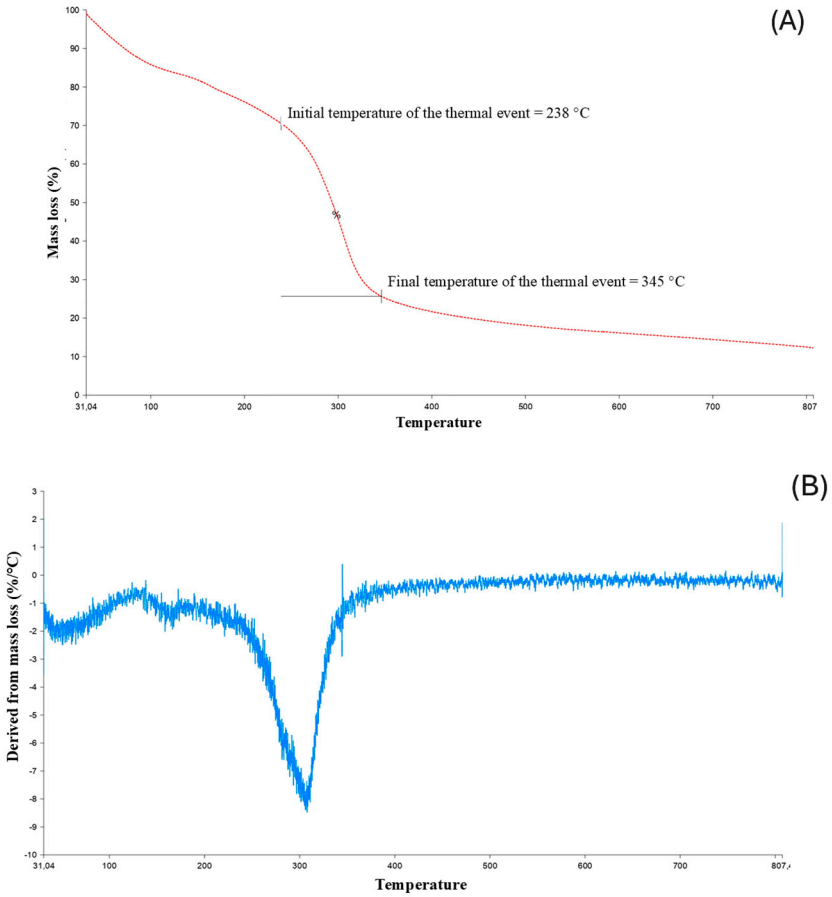

Figure 3. (**A**) Thermogravimetric analysis (TGA) curve showing the relationship between mass loss (%) and temperature (°C) in red; (**B**) derivative thermogravimetry (DTG) curve of the film in blue.

Fourier transform infrared spectroscopy (FTIR) analysis of I3 revealed characteristic bands associated with bioactive compounds typical of *Ilex paraguariensis* (Figure 4A). The broad band observed at ~3231 cm^{-1} is attributed to O–H stretching, characteristic of phenolic hydroxyl groups, mainly present in chlorogenic acids and flavonoids [38]. The band at ~2926 cm^{-1} is related to aliphatic C–H stretching, while the band at ~1596 cm^{-1} is attributed to C=C aromatic vibrations and/or conjugated C=O stretching, commonly associated with phenolic compounds and methylxanthines such as caffeine [46]. The bands located between 1400 and 1000 cm^{-1} are associated with C–O and C–O–C stretching, indicating the presence of esterified phenolics and soluble carbohydrates in the extract [38].

The FTIR spectrum of the film containing I3 (Figure 4B) showed the preservation of the main bands associated with the bioactive compounds, particularly the aromatic band at ~1597 cm^{-1}, indicating that phenolic compounds and methylxanthines remained structurally stable after film processing. In addition, characteristic bands of the starch–CMC polymeric matrix were clearly identified, including the broad O–H stretching band (~3200–3400 cm^{-1}), centered around ~3282 cm^{-1}, C–H stretching (~2920 cm^{-1}), and the C–O and C–O–C vibrations in the fingerprint region (~1140–1000 cm^{-1}), associated with glycosidic linkages and the polysaccharide backbone. Contributions from carboxylate groups ($–COO^{-}$) of CMC were also observed in the region of ~1600–1400 cm^{-1}, consistent with the band at ~1331 cm^{-1}. [38,46]. The shift in the O–H band to ~3282 cm^{-1}, together with changes in intensity and profile in the fingerprint region, indicates the occurrence of intermolecular interactions, mainly hydrogen bonding, between the hydroxyl groups of starch and CMC and the phenolic compounds present in the I3 extract. These changes suggest a modification in the hydrogen bonding network of the matrix, which may in-

fluence the organization and interactions of polymer chains [46]. The absence of new absorption bands indicates that no covalent interactions occurred between the extract and the polymeric matrix. However, the observed band shifts and intensity variations support the formation of molecular associations, confirming that the bioactive compounds were effectively incorporated into the film matrix. Overall, the FTIR results indicate good compatibility between the I3 extract and the starch–CMC matrix, which may contribute to the stability and functional performance of the developed films.

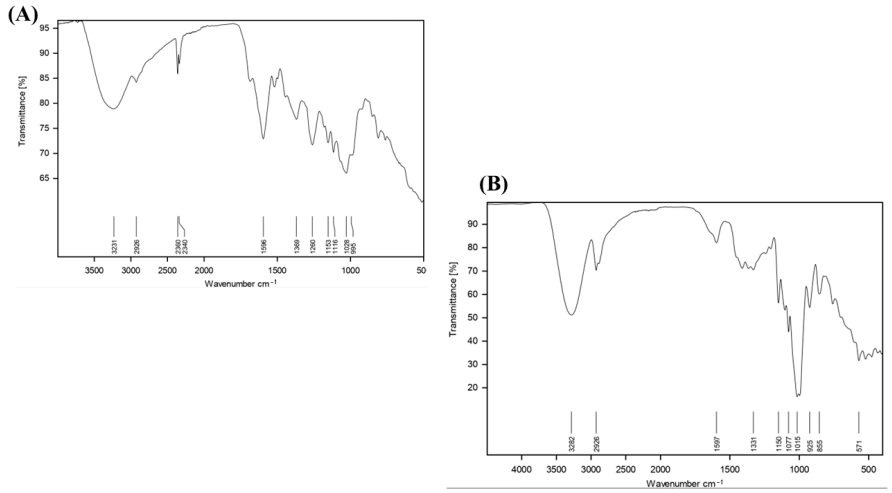

Figure 4. Fourier transform infrared spectroscopy (FTIR): (**A**) ice fraction 3–I3; (**B**) biopolymer film incorporated with the ice fraction 3.

The scanning electron microscopy (SEM) (Figure 5) shows that the film exhibits a homogeneous, continuous surface at 200× magnification (Figure 5A), indicating proper formation of the polymeric matrix during the film-forming process. At 500× magnification (Figure 5B), small particles are observed distributed across the film surface, likely associated with components of the starch. These particles did not lead to pronounced porosity or relevant structural defects, suggesting a satisfactory interaction between the I3 and the polymeric matrix. At higher magnification (1000×, Figure 5C), surface irregularities and microcracks become visible, which may be related to both the matrix composition and the conditions used during processing and analysis. This type of discontinuity can be favored by factors such as higher processing temperatures and lower plasticizer content, which increase material stiffness and, consequently, increase susceptibility to defect formation at the micrometric scale. In Figure 5D (400× magnification), the film thickness can be observed, and the measurements indicate a heterogeneous distribution along the analyzed cross-section. This variation may be attributed to the components in the polymeric matrix. Such behavior may be related to the I3's chemical complexity and the limited solubility of some of its constituents. Nevertheless, the absence of large-diameter structures or extensive agglomerations indicates that the dispersion of the I3 was sufficient to maintain matrix continuity, without compromising the structural integrity of the film. Similar behavior has been reported for biodegradable films containing plant extracts, in which increased surface heterogeneity and the presence of structures with varying dimensions across the film thickness are commonly observed, without necessarily impairing the overall structural properties when proper integration between matrix components occurs [47–49].

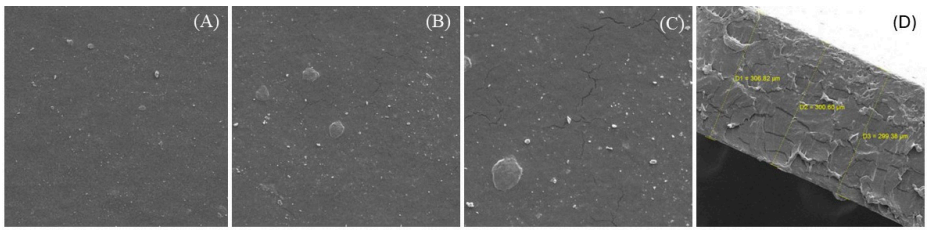

Figure 5. Scanning electron microscopy (SEM) micrographs: (**A**) film surface at 200× magnification (working distance = 1.04 mm); (**B**) film surface at 500× magnification (working distance = 415 µm); (**C**) film surface at 1000× magnification (working distance = 207 µm); (**D**) film cross-section showing thickness at 400× magnification (working distance = 519 µm).

3.5. Coloration Parameters and Intelligent Freshness Indicator

The film exhibited high luminance (L = 82.72 ± 0.55*), indicating a light, homogeneous surface. The *a** value (4.80 ± 0.32) showed a slight tendency toward reddish tones, while *b** (22.23 ± 1.30) confirmed the predominance of a yellowish coloration, characteristic of the incorporation of bioactive compounds from yerba mate. The opacity of 10.98% indicated that the material remained translucent, meeting the requirements of packaging systems that demand partial light protection. These results are consistent with those reported by Jamróz et al. [50], who observed *L** values between 73 and 78, *a** values from 3.9 to 9.2, and *b** values between 76 and 80 in films containing extract. Chen et al. [51] also observed that films enriched with phenolic extracts gain a reddish–yellow coloration very similar to that elaborated in the present manuscript.

Hoffmann et al. [5] reported that color differences between two samples become visually perceptible when the Δ*E* value exceeds 5.0. Based on the results presented in Table 2, the developed film showed Δ*E* values greater than 5 under all evaluated pH conditions, confirming visually detectable color changes. This response highlights the potential use of the film as a pH-sensitive indicator in intelligent food packaging systems, enabling rapid visual monitoring of quality changes associated with spoilage.

Table 2. Color parameters (CIELAB) and total color difference (Δ*E*) of the film under different pH conditions.

pH	*L**	*a**	*b**	Δ*E*
4	80.46 ^{a} ± 3.50	−1.74 ^{d} ± 0.02	16.95 ^{d} ± 2.90	8.70 ^{d} ± 0.50
7	74.72 ^{b} ± 2.11	−3.51 ^{c} ± 1.16	20.66 ^{c} ± 1.50	11.64 ^{c} ± 1.24
10	73.45 ^{b} ± 2.58	−4.14 ^{b} ± 1.87	28.98 ^{b} ± 3.15	14.54 ^{b} ± 2.10
12	64.83 ^{c} ± 1.36	−8.04 ^{a} ± 1.10	46.16 ^{a} ± 2.19	32.52 ^{a} ± 3.28

Results are expressed as the mean ± standard. $^{a, b, c, d}$ Within a column, different superscript lowercase letters denote significant differences ($p < 0.05$). Initial color parameters of film: L_0* = 82.72 ± 0.55; a_0* = 4.80 ± 0.32; b_0* = 22.23 ± 1.35.

As illustrated, the I3 (Figure 6A) and the film (Figure 6B) exhibit progressive color changes as pH increases, shifting from lighter yellowish tones under acidic and near-neutral conditions to more intense green–yellow hues in alkaline environments, particularly at pH 10 and 12.

This behavior can be attributed to chemical and structural changes in the main bioactive compounds present in yerba mate in response to pH variations. Previous studies report that pigments and phenolic compounds undergo electronic and structural rearrangements depending on the medium, as reflected in changes in the UV–Vis absorption profile and, consequently, in perceived color. Under alkaline conditions, the ionization of phenolic groups, combined with the relatively higher stability of chlorophylls, promotes increased absorption in the visible region, leading to more intense coloration [9,38,47,49,52].

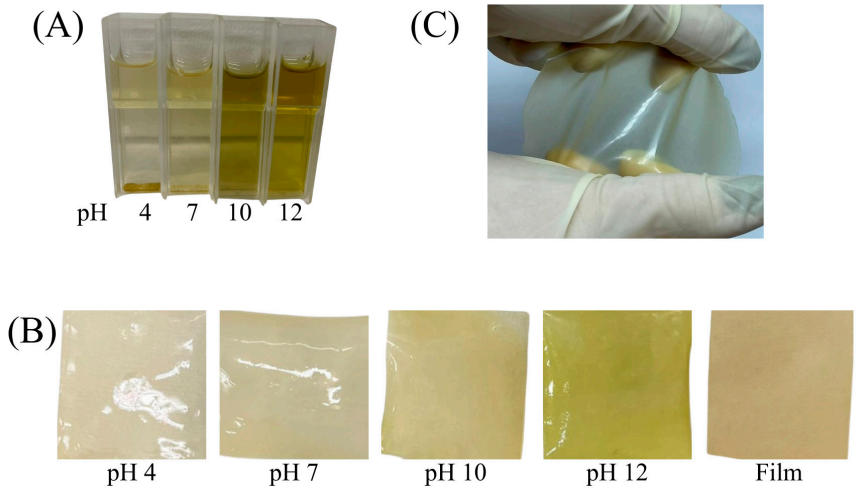

Figure 6. (**A**) Visual response of ice fraction 3 (I3) to pH variation at pH 4, 7, 10, and 12; (**B**) color differences observed in films containing I3 under different pH conditions (pH 4, 7, 10, and 12), compared with the film containing I3 without pH modification; (**C**) developed biopolymer film incorporating I3.

In addition to the direct effect of pH, the parameters used in preparing the yerba mate extract, such as extraction temperature and the contact time between the plant matrix and the solvent (water), also play a significant role in the solubilization of bioactive compounds. Total phenolics, chlorogenic acids, and flavonoids present in high concentrations in yerba mate contribute significantly to the chromatic response of the system [38,52–55].

The interaction between the chemical composition of the I3 and the surrounding medium explains the color differences observed across the evaluated pH range. These findings reinforce the potential of I3 as a functional component in polymeric matrices, particularly for the development of pH-responsive materials aimed at intelligent and environmentally sustainable applications [9,52,55]. Finally, the pH-dependent color transition is a hallmark of the bioactive compounds present in the I3 extract. Pure biopolymeric films are typically colorless and exhibit little chemical sensitivity, confirming that I3 acted as a smart functionalizing agent.

3.6. Biodegradability Test

The biodegradability test was performed by monitoring the degradation of the developed film through photographic records and mass loss. The biodegradability assay was conducted using a qualitative approach, in which the degradation of the produced films was monitored via periodic photographic documentation and mass loss measurements over time (Figure 7). Circular film specimens with a diameter of 10 cm were monitored for 45 days (Figure 7). Visual inspection revealed progressive deterioration of the material; by days 8, 12, and 24, the films had lost mechanical integrity and rigidity, indicating partial degradation. At 32 days, only small residual fragments of the material were observed, whereas at 45 days, the films had completely disintegrated under soil burial conditions. The loss of mass was progressive over the days of analysis. On day 8, 18%; on day 12, 27%; on day 24, 39%; on day 32, 78%; and on day 45, 100%.

The biodegradation mechanism may be described as occurring in three successive phases. Initially, soluble organic and inorganic components migrate from the film matrix into the surrounding soil. Subsequently, microbial colonization and enzymatic activity promote further degradation within the polymeric structure. In the final phase, macroscopic changes in the film's appearance, such as fragmentation and disintegration, become evident, culminating in complete degradation [5,56]. As we presented in this study, some in-

dependent studies describe the same three-phase biodegradation mechanism. For example, Wu et al. [57], Wang et al. [58], and Yu et al. [59] evaluated the biodegradability of microplastics in agricultural soils, studied the degradation of poly(butylene adipate-co-butylene terephthalate) (PBAT), and determined the mineralization and microbial utilization of poly(lactic acid) (PLA) microplastics in soil, respectively.

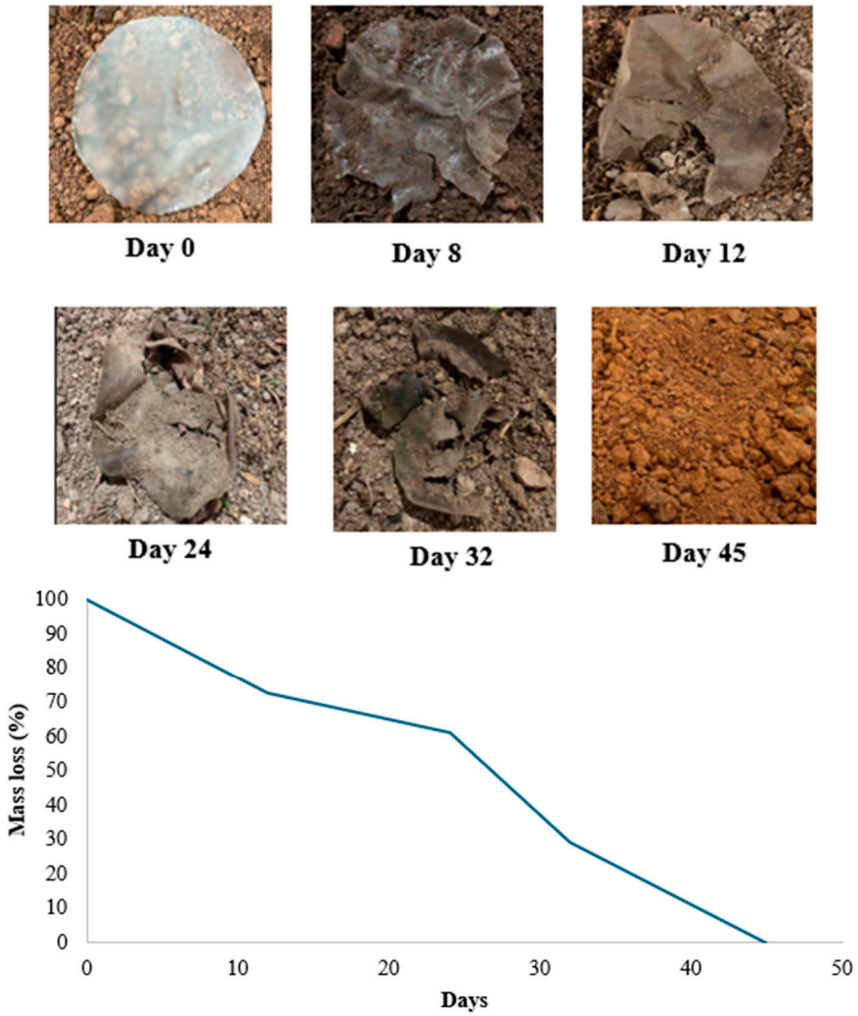

Figure 7. Soil biodegradability analysis of the film (day 0, 8, 12, 24, 32, and 45), and mass loss behavior.

Although a progressive mass loss was observed over time, culminating in the complete disappearance of the samples at 45 days, this result does not necessarily reflect exclusively microbial biodegradation. Given the relatively high water solubility of the developed films, a portion of the mass loss, particularly in the initial stages, may be attributed to dissolution or physical disintegration rather than to biological activity. This aspect is especially relevant in soil environments with inherent moisture, which can accelerate solubilization processes. Therefore, the results should be interpreted as indicative of disintegration under soil burial conditions, rather than definitive evidence of complete biodegradation. Complementary approaches, such as respirometric analyses (e.g., CO_2 evolution), enzyme activity measurements, and soil microbiome characterization, would be necessary to more rigorously distinguish between abiotic and biotic degradation mechanisms and to provide a more comprehensive assessment of the films' biodegradation behavior.

3.7. Total Phenolic Content and Antioxidant Activity

According to Table 3, the incorporation of the I3 obtained from the freeze concentration process of yerba mate extract into the film matrix resulted in a material with significant antioxidant potential, evidenced by both the total phenolic content and the high values obtained in the antioxidant capacity assays by DPPH and ABTS. The observed total phenolic content (1.01 ± 0.02 mg GAE g^{-1}) indicates that, although the ice fraction is often considered a less concentrated phase of the freeze concentration process, it preserves relevant amounts of bioactive compounds. Since the starch-CMC matrix does not possess intrinsic antioxidant capacity or phenolic compounds, the observed values (1.01 mg GAE/g and high DPPH/ABTS inhibition) are exclusively attributed to the bioactive compounds retained in the I3 fraction from yerba mate. This behavior can be attributed to the partial trapping of phenolic molecules in the ice matrix during crystal formation and growth, a phenomenon already described for aqueous systems rich in polyphenols subjected to controlled freezing processes [33,60].

Table 3. TPC and antioxidant activity of the biopolymeric film with ice fraction from the freeze concentration process of yerba mate extract.

Antioxidant Parameter	Result
Total phenolic content (mg GAE g^{-1})	1.01 ± 0.02
DPPH (µmol TE g^{-1})	2094.00 ± 5.00
ABTS + (µmol TE g^{-1})	1610.00 ± 8.00

When compared to values reported in the literature for active biodegradable films incorporating plant extracts, the results obtained in this study are competitive. Films based on polysaccharides, such as starch and chitosan, with added conventional yerba mate extract, generally present total phenolic contents ranging from 0.30 to 0.85 mg GAE g^{-1}, depending on the extract concentration, the extraction method, and the compatibility with the polymeric matrix. Thus, the observed values suggest that the reuse of the I3 from freeze concentration constitutes an efficient alternative for the valorization of by-products, without compromising the phenolic content of the final material [38,61].

The antioxidant activity evaluated by the DPPH method was 2094.00 ± 5.00 µmol TE g^{-1}, indicating a high capacity to scavenge free radicals. Values of this magnitude are higher than those reported for most active films developed with plant extracts, which frequently show activity below 1000 µmol TE g^{-1} [62]. Studies involving biodegradable films incorporating conventional yerba mate extract report intermediate values, generally between 1200 and 1600 µmol TE g^{-1}, mainly attributed to the presence of chlorogenic acids and their derivatives [63]. Thus, the results suggest that freeze concentration, even when considering the ice fraction, contributes to the preservation of highly reactive compounds against the DPPH radical.

Consistent results were observed in the ABTS assay, with a value of 1610.00 ± 8.00 µmol TE g^{-1}. The ABTS method shows greater sensitivity to hydrophilic and lipophilic antioxidant compounds, being widely used for the functional characterization of active films [62,64]. To better contextualize the antioxidant performance of the developed film, it is important to compare the present results with those reported for recent active packaging systems. The DPPH (2094.00 ± 5.00 µmol TE g^{-1}) and ABTS (1610.00 ± 8.00 µmol TE g^{-1}) values obtained in this study were markedly higher than those reported for several recently developed biodegradable films containing natural antioxidants. For example, Spirulina-incorporated biopolymer films showed antioxidant activity of up to 320.08 µmol TE g^{-1} [65], while emulsified collagen/Bambara groundnut protein films reached approximately 60.45 µmol TE g^{-1} by DPPH [66]. In oregano-essential-

oil-based films, even lower values were reported, with 6.07 μmol TE g^{-1} for DPPH and 6.64 μmol TE g^{-1} for ABTS [67].

Although direct comparisons should be interpreted with caution due to differences in analytical methods, expression of results, and film composition, these data indicate that the film developed in the present study is positioned in the upper range of antioxidant performance among recent active packaging materials. This behavior reinforces that the I3 fraction from freeze concentration, despite being a residual stream, retained a sufficient concentration of phenolic compounds to provide a strong radical-scavenging capacity when incorporated into the polymeric matrix. These findings highlight the potential of freeze concentration by-products as competitive alternatives to conventional plant extracts in active packaging systems.

The difference between the values obtained in the DPPH and ABTS methods is expected and is related to differences in reaction mechanisms and the selectivity of the radicals employed, with higher responses commonly observed in the DPPH for systems rich in simple phenols, such as those predominant in yerba mate [68,69].

The direct relationship between total phenolic content and the high antioxidant activity observed in this study is consistent with studies reporting a significant positive correlation between these variables in active biodegradable films, indicating that phenolic compounds play a central role in the material's antioxidant functionality. Furthermore, the incorporation of these compounds into the polymeric matrix may favor their gradual release, expanding the potential for application in active packaging systems [70–72]. Several manuscripts clearly demonstrate that incorporating antioxidant and phenolic compounds into polymeric matrices enables their gradual or sustained release, thereby directly corroborating their use in active packaging systems. These studies describe diffusion-controlled, matrix-regulated release, showing that phenolic compounds remain protected within the polymeric network and are progressively released, providing prolonged antioxidant functionality. Examples include studies on grape by-product phenolics in polymer matrices (Silva et al. [73]), phenolic acids in gelatin coatings (Benbettaieb et al. [74]) and in biobased films from *Annurca* apple-processing waste (Qamar et al. [75]), and açaí powder-enriched biodegradable starch films (Maciel et al. [76]).

Based on the results presented, the developed film can be characterized as a functional biopolymeric film, since it exhibits high antioxidant activity, with the potential to retard oxidative processes in sensitive foods. Moreover, the use of the ice fraction from the freeze concentration process represents a sustainable strategy for valorizing by-products, aligned with the principles of the circular economy and current trends in the development of functional and environmentally responsible materials for the food industry [33].

4. Conclusions

This study demonstrated the potential for reusing residues generated during the block freeze-concentration of yerba mate extract through the incorporation of the ice fraction into a biodegradable biopolymer film. The freeze-concentration process showed progressive efficiency across the stages, with the third stage presenting the highest concentration factor and process efficiency. Although considered a dilute phase, the ice fraction retained relevant amounts of bioactive compounds, enabling its application as a functional component in the polymeric matrix.

The developed film exhibited suitable physicochemical and mechanical properties for biodegradable packaging applications, including uniform thickness, moderate tensile strength, and good flexibility. Structural analyses confirmed the successful incorporation of yerba mate compounds (ice fraction 3) into the film, with preservation of phenolic structures and homogeneous distribution within the matrix. In addition, the material showed

significant antioxidant activity and a colorimetric response to pH variations, indicating its potential as a responsive material with possible application in active and intelligent packaging systems. The complete biodegradation observed in the soil test further supports its environmental compatibility. A limitation of this study is the absence of a control film prepared under identical experimental conditions (i.e., a starch/CMC matrix without the I3 fraction). Although the base matrix is reported to lack antioxidant and pH-sensitive properties, its physical and mechanical behavior may vary depending on processing conditions. Thus, while the results are consistent with the incorporation of the I3 fraction, they should be interpreted with prudence. Future studies should include an appropriate control film to enable a more robust assessment of the active fraction's contribution.

The results indicate that residues from freeze-concentration can be revalorized as functional additives in biodegradable polymer systems, contributing to the development of more sustainable and value-added materials for food packaging applications. This approach enables the utilization of underexplored fractions of the process, adding value to by-products while reducing waste. These findings demonstrate the feasibility of using yerba mate ice fractions as active ingredients, providing strong evidence of their role in developing smart and antioxidant packaging.

From an industrial perspective, the incorporation of these residues represents a promising strategy for the development of new materials and functional ingredients, aligned with the growing demand for sustainable solutions and circular economy principles. The potential application of these materials at an industrial scale reinforces their relevance for the food packaging sector, particularly in the development of active systems and materials with responsive properties that may be further explored as intelligent packaging. However, additional studies are required to confirm this applicability, including the evaluation of film performance in different food matrices and under various storage conditions, as well as comparisons with control samples without the addition of the I3 fraction. Future research should also address the scalability of the process to better understand its industrial feasibility and practical application in real food systems.

Author Contributions: Conceptualization, A.C.F.C., C.K.d.S. and E.S.P.; methodology, A.C.F.C. and J.P.; software, A.A.P. and K.M.; validation, A.C.F.C. and J.P.; formal analysis, A.C.F.C. and J.P.; investigation, A.C.F.C. and J.P.; resources, D.R.M.A., J.S.d.G. and C.V.H.; data curation, A.C.F.C., A.A.P. and K.M.; writing—original draft preparation, A.C.F.C., A.A.P. and K.M.; writing—review and editing, A.C.F.C. and P.T.; visualization, E.S.P.; supervision, E.S.P.; project administration, E.S.P.; funding acquisition, J.S.d.G., C.K.d.S. and E.S.P. All authors have read and agreed to the published version of the manuscript.

Funding: This research was funded by the National Council for Scientific and Technological Development (CNPq, Brazil) [303069/2022-8; 174429/2023-1; 302867/2023-6], and by a scholarship from the Coordination for the Improvement of Higher Education Personnel (CAPES, Brazil—Finance Code 001). Financial support was also provided by the Foundation for Research Support of the State of Rio de Janeiro (FAPERJ) and the Foundation for Research and Innovation Support of the State of Santa Catarina (FAPESC) (TO2025TR001604), as well as the Ministry of Science, Technology and Innovation (MCTI), Brazil.

Data Availability Statement: The original contributions presented in the study are included in the article; further inquiries can be directed to the corresponding authors.

Acknowledgments: The authors thank CAPES (Coordination of Improvement of Higher Education Personnel, Brazil—Finance Code 001) and CNPq (National Council for Scientific and Technological Development, Brazil) for the scholarships.

Conflicts of Interest: Author Cristiane Vieira Helm is employed by Brazilian Agricultural Research Corporation. The authors declare that the research was conducted in the absence of any commercial or financial relationships that could be construed as a potential conflict of interest. The company had no role in the design of the study, the collection, analysis, or interpretation of data, the writing of the manuscript, or the decision to publish the results.

References

1. Dantas, M.P.; de Oliveira, C.R.S.; Ueda Yamaguchi, N.; da Silva Júnior, A.H.; Peralta, R.M.; Bracht, A.; Corrêa, R.C.G. Pathways in Agro-Industrial Waste Upcycling: A Review of Sustainable Textile Innovations and Economic Perspectives. *Plants* **2025**, *14*, 3574. [CrossRef]
2. Islam, M.; Xayachak, T.; Haque, N.; Lau, D.; Bhuiyan, M.; Pramanik, B.K. Impact of Bioplastics on Environment from Its Production to End-of-Life. *Process Saf. Environ. Prot.* **2024**, *188*, 151–166. [CrossRef]
3. Haq, F.; Kiran, M.; Khan, I.A.; Mehmood, S.; Aziz, T.; Haroon, M. Exploring the Pathways to Sustainability: A Comprehensive Review of Biodegradable Plastics in the Circular Economy. *Mater. Today Sustain.* **2025**, *29*, 101067. [CrossRef]
4. Mueller, E.; Hoffmann, T.G.; Schmitz, F.R.W.; Helm, C.V.; Roy, S.; Bertoli, S.L.; de Souza, C.K. Development of Ternary Polymeric Films Based on Cassava Starch, Pea Flour and Green Banana Flour for Food Packaging. *Int. J. Biol. Macromol.* **2024**, *256*, 128436. [CrossRef] [PubMed]
5. Hoffmann, T.G.; Angioletti, B.L.; Bertoli, S.L.; de Souza, C.K. Intelligent PH-Sensing Film Based on Jaboticaba Peels Extract Incorporated on a Biopolymeric Matrix. *J. Food Sci. Technol.* **2022**, *59*, 1001–1010. [CrossRef] [PubMed]
6. Kumar, A.; Kumar, A.; Wei, S.; Chopra, S.; Rudra, S.G.; Rabbani, A. Biodegradable and Smart Packaging Films for Food Quality and Safety: A Review. *Appl. Food Res.* **2025**, *5*, 101491. [CrossRef]
7. Rani, J.; Gulia, V.; Dhull, S.S.; Beniwal, D.; Deepali. Active Packaging for Convenience Foods: Enhancing Quality and Sustainability. In *Green Materials for Active Food Packaging*; Springer Nature: Berlin/Heidelberg, Germany, 2025; pp. 455–482.
8. Da Rocha, J.; Mustafa, S.K.; Jagnandan, A.; Ahmad, M.A.; Rebezov, M.; Shariati, M.A.; Krebs de Souza, C. Development of Active and Biodegradable Film of Ternary-Based for Food Application. *Potravin. Slovak J. Food Sci.* **2023**, *17*, 148–158. [CrossRef]
9. Farias, N.S.d.; Silva, B.; de Oliveira Costa, A.C.; Müller, C.M.O. Alginate Based Antioxidant Films with Yerba Mate (*Ilex paraguariensis* St. Hil.): Characterization and Kinetics of Phenolic Compounds Release. *Food Packag. Shelf Life* **2021**, *28*, 100548. [CrossRef]
10. Mesquita, M.; Santos, E.; Kassuya, C.A.; Salvador, M.J. Chimarrão, Terere and Mate-Tea in Legitimate Technology Modes of Preparation and Consume: A Comparative Study of Chemical Composition, Antioxidant, Anti-Inflammatory and Anti-Anxiety Properties of the Mostly Consumed Beverages of *Ilex paraguariensis* St. Hil. *J. Ethnopharmacol.* **2021**, *279*, 114401. [CrossRef]
11. Song, Y.; Cao, J.; Cao, F.; Su, E. A Systematic Review on the Yerba Mate (*Ilex paraguariensis* A. St. Hil.). *J. Food Compos. Anal.* **2025**, *142*, 107466. [CrossRef]
12. Zhang, Q.-W.; Lin, L.-G.; Ye, W.-C. Techniques for Extraction and Isolation of Natural Products: A Comprehensive Review. *Chin. Med.* **2018**, *13*, 20. [CrossRef]
13. Boaventura, B.C.B.; Murakami, A.N.N.; Prudêncio, E.S.; Maraschin, M.; Murakami, F.S.; Amante, E.R.; Amboni, R.D.d.M.C. Enhancement of Bioactive Compounds Content and Antioxidant Activity of Aqueous Extract of Mate (*Ilex paraguariensis* A. St. Hil.) through Freeze Concentration Technology. *Food Res. Int.* **2013**, *53*, 686–692. [CrossRef]
14. Pérez-Bermúdez, I.; Castillo-Suero, A.; Jara-Leiva, C.; Cortés-Valdivia, A.; Rojas-Rojas, K.; García-Rojas, V.; Opazo-Navarrete, M.; Guerra-Valle, M.; Petzold, G.; Orellana-Palma, P. Effect of Block Freeze Concentration on Bioactive Compound Content and Antioxidant Capacity When Applied to Peppermint (*Mentha piperita* L.) Infusion. *Antioxidants* **2025**, *14*, 129. [CrossRef]
15. Alves, F.E.d.S.B.; Scheer, A.d.P. Yerba Mate (*Ilex paraguariensis*), Science, Technology and Health: A Systematic Review on Research, Recent Advances and Possible Paths for Future Studies. *S. Afr. J. Bot.* **2024**, *168*, 573–587. [CrossRef]
16. Casagranda, M.C.; Silva, R.B.d.; Morisso, F.D.P.; Santana, R.M.C. Exploring the Plasticizing Effect of Yerba Mate Extract and Malic Acid in Potato Starch-Based Films. *Mater. Res.* **2025**, *28*, e20250073. [CrossRef]
17. Carvalho, A.C.F.; Ghosh, S.; Hoffmann, T.G.; Prudêncio, E.S.; de Souza, C.K.; Roy, S. Valuing Agro-Industrial Waste in the Development of Sustainable Food Packaging Based on the System of a Circular Bioeconomy: A Review. *Clean. Waste Syst.* **2025**, *11*, 100275. [CrossRef]
18. Carvalho, A.C.F.; Hoffmann, T.G.; Helm, C.V.; Prudêncio, E.S.; Roy, S.; de Souza, C.K. Smart Biopolymer Based on Rice Husk Extracts and Pinhão Failure Applied as an Interlayer for Sliced Mozzarella Cheese. *J. Vinyl Addit. Technol.* **2025**, *31*, 1233–1246. [CrossRef]
19. Soares, M.; Faria, L.; Miranda, T.; Pereira, E.; Vilarinho, C.; Carvalho, J. The Potential of Agri-Food Waste to Solve Construction's Environmental Problems: A Review. *Clean. Circ. Bioecon.* **2025**, *10*, 100138. [CrossRef]

20. Bremer Boaventura, B.C.; da Silva, E.L.; Liu, R.H.; Prudêncio, E.S.; Di Pietro, P.F.; Becker, A.M.; Amboni, R.D.d.M.C. Effect of Yerba Mate (*Ilex paraguariensis* A. St. Hil.) Infusion Obtained by Freeze Concentration Technology on Antioxidant Status of Healthy Individuals. *LWT-Food Sci. Technol.* **2015**, *62*, 948–954. [CrossRef]
21. Negrão Murakami, A.N.; de Mello Castanho Amboni, R.D.; Prudêncio, E.S.; Amante, E.R.; de Moraes Zanotta, L.; Maraschin, M.; Cunha Petrus, J.C.; Teófilo, R.F. Concentration of Phenolic Compounds in Aqueous Mate (*Ilex paraguariensis* A. St. Hil) Extract through Nanofiltration. *LWT-Food Sci. Technol.* **2011**, *44*, 2211–2216. [CrossRef]
22. Canella, M.H.M.; Munoz, I.d.B.; Pinto, S.S.; de Liz, G.R.; Muller, C.M.O.; Amboni, R.D.d.M.C.; Prudencio, E.S. Use of Concentrated Whey by Freeze Concentration Process to Obtain a Symbiotic Fermented Lactic Beverage. *Adv. J. Food Sci. Technol.* **2018**, *14*, 56–68. [CrossRef]
23. Aider, M.; Ounis, W. Ben Skim Milk Cryoconcentration as Affected by the Thawing Mode: Gravitational vs. Microwave-assisted. *Int. J. Food Sci. Technol.* **2012**, *47*, 195–202. [CrossRef]
24. Finardi, S.; Hoffmann, T.G.; Angioletti, B.L.; Mueller, E.; Lazzaris, R.S.; Bertoli, S.L.; Hlebová, M.; Khayrullin, M.; Nikolaeva, N.; Shariati, M.A.; et al. Development and Application of Antioxidant Coating on *Fragaria* spp. Stored under Isothermal Conditions. *J. Microbiol. Biotechnol. Food Sci.* **2022**, *11*, e5432. [CrossRef]
25. Mueller, E.; Gabriela Hoffmann, T.; Ferreira Carvalho, A.C.; Meinert, C.; Vieira Helm, C.; Priyadarshi, R.; Krebs de Souza, C. Smart Biodegradable Packaging Film from Cassava Starch, Pea Flour, and Yerba Mate Extract. *J. Packag. Technol. Res.* **2025**, *10*, 63–78. [CrossRef]
26. Jorge, A.M.S.; Gaspar, M.C.; Henriques, M.H.F.; Braga, M.E.M. Edible Films Produced from Agrifood By-Products and Wastes. *Innov. Food Sci. Emerg. Technol.* **2023**, *88*, 103442. [CrossRef]
27. *ASTM D882*; Standard Test Method for Tensile Properties of Thin Plastic Sheeting. ASTM International: West Conshohocken, PA, USA, 2018.
28. Baltacıoğlu, H.; Baltacıoğlu, C.; Okur, I.; Tanrıvermiş, A.; Yalıç, M. Optimization of Microwave-Assisted Extraction of Phenolic Compounds from Tomato: Characterization by FTIR and HPLC and Comparison with Conventional Solvent Extraction. *Vib. Spectrosc.* **2021**, *113*, 103204. [CrossRef]
29. Singleton, V.L.; Rossi, J.A. Colorimetry of Total Phenolics with Phosphomolybdic-Phosphotungstic Acid Reagents. *Am. J. Enol. Vitic.* **1965**, *16*, 144–158. [CrossRef]
30. Carvalho, A.C.F.; Vieira, G.M.N.; Prestes, A.A.; Marafon, K.; de Souza, C.K.; Andrade, D.R.M.; Helm, C.V.; de Gois, J.S.; Prudêncio, E.S. Development and Characterization of Dairy Compound with Goat Milk Powder and Rice Flour. *Processes* **2025**, *13*, 2324. [CrossRef]
31. Brand-Williams, W.; Cuvelier, M.E.; Berset, C. Use of a Free Radical Method to Evaluate Antioxidant Activity. *LWT-Food Sci. Technol.* **1995**, *28*, 25–30. [CrossRef]
32. Re, R.; Pellegrini, N.; Proteggente, A.; Pannala, A.; Yang, M.; Rice-Evans, C. Antioxidant Activity Applying an Improved ABTS Radical Cation Decolorization Assay. *Free Radic. Biol. Med.* **1999**, *26*, 1231–1237. [CrossRef]
33. Prestes, A.A.; Marafon, K.; Carvalho, A.C.F.; Andrade, D.R.M.; Helm, C.V.; de Gois, J.S.; Monteiro Wanderley, B.R.d.S.; Amboni, R.D.d.M.C.; Prudencio, E.S. The Functional Carbonated Beverage Properties of Guabiroba Juice Using the Ice Fraction from Gravitational Block Freeze Concentration. *Processes* **2024**, *12*, 2235. [CrossRef]
34. Bredun, M.A.; Prestes, A.A.; Panceri, C.P.; Prudêncio, E.S.; Burin, V.M. Bioactive Compounds Recovery by Freeze Concentration Process from Winemaking By-Product. *Food Res. Int.* **2023**, *173*, 113220. [CrossRef]
35. Marafon, K.; Pereira-Coelho, M.; da Silva Haas, I.C.; da Silva Monteiro Wanderley, B.R.; de Gois, J.S.; Vitali, L.; Luna, A.S.; Canella, M.H.M.; Hernández, E.; de Mello Castanho Amboni, R.D.; et al. An Opportunity for Acerola Pulp (*Malpighia emarginata* DC) Valorization Evaluating Its Performance during the Block Cryoconcentration by Physicochemical, Bioactive Compounds, HPLC–ESI-MS/MS, and Multi-Elemental Profile Analysis. *Food Res. Int.* **2024**, *176*, 113793. [CrossRef]
36. Prestes, A.A.; Andrade, D.R.M.; Canella, M.H.M.; Haas, I.C.d.S.; Helm, C.V.; de Gois, J.S.; Block, J.M.; Wanderley, B.R.d.S.M.; Amboni, R.D.d.M.C.; Cruz, A.G.d.; et al. The Addition of Concentrated Cold-Pressed Guabiroba Juice to Yogurts: Effects on the Physicochemical Analyses, Antioxidant Activity, Carotenoid Content, Total Phenolic Compounds, and Mineral Profile. *Processes* **2024**, *12*, 1915. [CrossRef]
37. Medina Jaramillo, C.; Gutiérrez, T.J.; Goyanes, S.; Bernal, C.; Famá, L. Biodegradability and Plasticizing Effect of Yerba Mate Extract on Cassava Starch Edible Films. *Carbohydr. Polym.* **2016**, *151*, 150–159. [CrossRef]
38. Ceballos, R.L.; Ochoa-Yepes, O.; Goyanes, S.; Bernal, C.; Famá, L. Effect of Yerba Mate Extract on the Performance of Starch Films Obtained by Extrusion and Compression Molding as Active and Smart Packaging. *Carbohydr. Polym.* **2020**, *244*, 116495. [CrossRef] [PubMed]
39. Leon-Bejarano, M.; Durmus, Y.; Ovando-Martínez, M.; Simsek, S. Physical, Barrier, Mechanical, and Biodegradability Properties of Modified Starch Films with Nut By-Products Extracts. *Foods* **2020**, *9*, 226. [CrossRef]
40. Bishnoi, A.; Chandla, N.K.; Talwar, G.; Khatkar, S.K.; Sharma, A. Mechanical Strength, Solubility, and Functional Studies of Developed Composite Biopolymeric Film. *J. Food Process. Preserv.* **2023**, *2023*, 5108490. [CrossRef]

41. Bertuzzi, M.A.; Castro Vidaurre, E.F.; Armada, M.; Gottifredi, J.C. Water Vapor Permeability of Edible Starch Based Films. *J. Food Eng.* **2007**, *80*, 972–978. [CrossRef]
42. Regmi, S.; Janaswamy, S. Biodegradable Films from Soyhull Cellulosic Residue with UV Protection and Antioxidant Properties Improve the Shelf-Life of Post-Harvested Raspberries. *Food Chem.* **2024**, *460*, 140672. [CrossRef] [PubMed]
43. Żołek-Tryznowska, Z.; Kałuża, A. The Influence of Starch Origin on the Properties of Starch Films: Packaging Performance. *Materials* **2021**, *14*, 1146. [CrossRef]
44. Lopes, A.I.; Melo, A.; Afonso, T.B.; Silva, S.; Barros, L.; Tavaria, F.K.; Pintado, M. Alginate Edible Films Containing Essential Oils: Characterization and Bioactive Potential. *Polymers* **2025**, *17*, 1188. [CrossRef]
45. Karnwal, A.; Rauf, A.; Jassim, A.Y.; Selvaraj, M.; Al-Tawaha, A.R.M.S.; Kashyap, P.; Kumar, D.; Malik, T. Advanced Starch-Based Films for Food Packaging: Innovations in Sustainability and Functional Properties. *Food Chem. X* **2025**, *29*, 102662. [CrossRef]
46. Aliabadi, M.; Chee, B.S.; Matos, M.; Cortese, Y.J.; Nugent, M.J.D.; de Lima, T.A.M.; Magalhães, W.L.E.; de Lima, G.G. Yerba Mate Extract in Microfibrillated Cellulose and Corn Starch Films as a Potential Wound Healing Bandage. *Polymers* **2020**, *12*, 2807. [CrossRef]
47. Gómez-Bachar, L.; Vilcovsky, M.; González-Seligra, P.; Famá, L. Effects of PVA and Yerba Mate Extract on Extruded Films of Carboxymethyl Cassava Starch/PVA Blends for Antioxidant and Mechanically Resistant Food Packaging. *Int. J. Biol. Macromol.* **2024**, *268*, 131464. [CrossRef]
48. Sanchez, L.M.; de Haro, J.; Domínguez, E.; Rodríguez, A.; Heredia, A.; Benítez, J.J. Revalorization of Yerba Mate Residues: Biopolymers-Based Films of Dual Wettability as Potential Mulching Materials. *Polymers* **2024**, *16*, 815. [CrossRef] [PubMed]
49. Sirbu, E.-E.; Dinita, A.; Tănase, M.; Portoacă, A.-I.; Bondarev, A.; Enascuta, C.-E.; Calin, C. Influence of Plasticizers Concentration on Thermal, Mechanical, and Physicochemical Properties on Starch Films. *Processes* **2024**, *12*, 2021. [CrossRef]
50. Jamróz, E.; Kulawik, P.; Guzik, P.; Duda, I. The Verification of Intelligent Properties of Furcellaran Films with Plant Extracts on the Stored Fresh Atlantic Mackerel during Storage at 2 °C. *Food Hydrocoll.* **2019**, *97*, 105211. [CrossRef]
51. Chen, Y.; Xu, L.; Wang, Y.; Chen, Z.; Zhang, M.; Chen, H. Characterization and Functional Properties of a Pectin/Tara Gum Based Edible Film with Ellagitannins from the Unripe Fruits of *Rubus chingii* Hu. *Food Chem.* **2020**, *325*, 126964. [CrossRef]
52. Silveira Hornung, P.; Ávila, S.; Apea-Bah, F.B.; Liu, J.; Lopes Teixeira, G.; Hoffmann Ribani, R.; Beta, T. Sustainable Use of *Ilex paraguariensis* Waste in Improving Biodegradable Corn Starch Films' Mechanical, Thermal and Bioactive Properties. *J. Polym. Environ.* **2020**, *28*, 1696–1709. [CrossRef]
53. Rezzani, G.D.; Salvay, A.G.; Peltzer, M.A. Yerba Mate and Water Kefir Grain Films for Food Preservation and Freshness Indicators. *Food Bioprocess Technol.* **2025**, *18*, 2781–2794. [CrossRef]
54. Balbinot-Alfaro, E.; Craveiro, D.V.; Lima, K.O.; Costa, H.L.G.; Lopes, D.R.; Prentice, C. Intelligent Packaging with PH Indicator Potential. *Food Eng. Rev.* **2019**, *11*, 235–244. [CrossRef]
55. Saraiva, B.R.; Vital, A.C.P.; Anjo, F.A.; Ribas, J.C.R.; Matumoto Pintro, P.T. Effect of Yerba Mate (*Ilex paraguariensis* A. St.-Hil.) Addition on the Functional and Technological Characteristics of Fresh Cheese. *J. Food Sci. Technol.* **2019**, *56*, 1256–1265. [CrossRef]
56. Reichert, A.A.; De Freitas, T.C.; Alano, J.H.; Dantas, A.D.O. Evaluation of Phytotoxicity and Biodegradation of Cellulose Reinforced Starch Biocomposites. *Cellul. Chem. Technol.* **2022**, *56*, 807–814. [CrossRef]
57. Wu, J.; Gao, J.; Pei, Y.; Luo, K.; Yang, W.; Wu, J.; Yue, X.; Wen, J.; Luo, Y. Microplastics in Agricultural Soils: A Comprehensive Perspective on Occurrence, Environmental Behaviors and Effects. *Chem. Eng. J.* **2024**, *489*, 151328. [CrossRef]
58. Wang, Y.; Liu, Q.; Xie, C.-H.; Zhao, R.-T.; Tang, Q.-X.; Han, D.-F.; Xia, Y.-N.; Cui, J.-X.; Yan, C.-R.; He, W.-Q. Bridging the Knowledge Gap: From Poly(Butylene Adipate-Co-Terephthalatebutylene) Degradation to CO_2-Generating Mineralization under the Synergistic Effect of Bacteria and Fungi. *J. Hazard. Mater.* **2025**, *494*, 138643. [CrossRef]
59. Yu, Y.; Lin, S.; Sarkar, B.; Wang, J.; Liu, X.; Wang, D.; Ge, T.; Li, Y.; Zhu, B.; Yao, H. Mineralization and Microbial Utilization of Poly(Lactic Acid) Microplastic in Soil. *J. Hazard. Mater.* **2024**, *476*, 135080. [CrossRef]
60. Casas-Forero, N.; Orellana-Palma, P.; Petzold, G. Influence of Block Freeze Concentration and Evaporation on Physicochemical Properties, Bioactive Compounds and Antioxidant Activity in Blueberry Juice. *Food Sci. Technol.* **2020**, *40*, 387–394. [CrossRef]
61. Zhu, F. Starch Based Films and Coatings for Food Packaging: Interactions with Phenolic Compounds. *Food Res. Int.* **2025**, *204*, 115758. [CrossRef]
62. Martins, V.F.R.; Lopes, A.I.; Machado, M.; Costa, E.M.; Ribeiro, T.B.; Poças, F.; Pintado, M.; Morais, R.M.S.C.; Morais, A.M.M.B. Biodegradable Films with Polysaccharides, Proteins, and Bioactive Compounds from *Lobosphaera* sp.: Antioxidant and Antimicrobial Activities. *Foods* **2025**, *14*, 1327. [CrossRef] [PubMed]
63. Ali, A.; Ahmed, S. Eco-Friendly Natural Extract Loaded Antioxidative Chitosan/Polyvinyl Alcohol Based Active Films for Food Packaging. *Heliyon* **2021**, *7*, e06550. [CrossRef]
64. Lopes, A.I.; Melo, A.; Caleja, C.; Pereira, E.; Finimundy, T.C.; Afonso, T.B.; Silva, S.; Ivanov, M.; Soković, M.; Tavaria, F.K.; et al. Evaluation of Antimicrobial and Antioxidant Activities of Alginate Edible Coatings Incorporated with Plant Extracts. *Coatings* **2023**, *13*, 1487. [CrossRef]

65. Nakamoto, M.M.; Oliveira-Filho, J.G.; Assis, M.; Braga, A.R.C. *Spirulina*-Incorporated Biopolymer Films for Antioxidant Food Packaging. *Processes* **2025**, *13*, 4037. [CrossRef]
66. Awal, M.S.; Benjakul, S.; Prodpran, T.; Nilsuwan, K. Properties of Emulsion Co-Precipitated Collagen/Bambara Groundnut Protein-Based Film as Influenced by Basil Essential Oil and Soy Lecithin. *Polymers* **2025**, *17*, 1139. [CrossRef]
67. Uribe-Cruz, G.; Flores-Córdova, M.A.; Soto-Caballero, M.C.; Salas-Salazar, N.A.; Rodríguez-Roque, M.J.; Acosta-Muñiz, C.H.; Romero-Bastida, C.A.; Zamudio-Flores, P.B. Evaluation of the Effect of Oregano Essential Oil and Emulsifier Ratio on the Physicochemical, Mechanical, and Antioxidant Properties of Corn Starch Films Based on Gel Matrices. *Gels* **2025**, *11*, 760. [CrossRef]
68. Godlewska, K.; Pacyga, P.; Najda, A.; Michalak, I. Investigation of Chemical Constituents and Antioxidant Activity of Biologically Active Plant-Derived Natural Products. *Molecules* **2023**, *28*, 5572. [CrossRef] [PubMed]
69. Rumpf, J.; Burger, R.; Schulze, M. Statistical Evaluation of DPPH, ABTS, FRAP, and Folin-Ciocalteu Assays to Assess the Antioxidant Capacity of Lignins. *Int. J. Biol. Macromol.* **2023**, *233*, 123470. [CrossRef]
70. La Fuente, C.I.A.; Maniglia, B.C.; Tadini, C.C. Biodegradable Polymers: A Review about Biodegradation and Its Implications and Applications. *Packag. Technol. Sci.* **2023**, *36*, 81–95. [CrossRef]
71. Pan, J.; Li, C.; Liu, J.; Jiao, Z.; Zhang, Q.; Lv, Z.; Yang, W.; Chen, D.; Liu, H. Polysaccharide-Based Packaging Coatings and Films with Phenolic Compounds in Preservation of Fruits and Vegetables—A Review. *Foods* **2024**, *13*, 3896. [CrossRef]
72. Ordoñez, R.; Atarés, L.; Chiralt, A. Biodegradable Active Materials Containing Phenolic Acids for Food Packaging Applications. *Compr. Rev. Food Sci. Food Saf.* **2022**, *21*, 3910–3930. [CrossRef] [PubMed]
73. Silva, M.E.d.S.; Grisi, C.V.B.; Silva, S.P.d.; Madruga, M.S.; Silva, F.A.P.d. The Technological Potential of Agro-Industrial Residue from Grape Pulping (*Vitis* spp.) for Application in Meat Products: A Review. *Food Biosci.* **2022**, *49*, 101877. [CrossRef]
74. Benbettaieb, N.; Mlaouah, E.; Moundanga, S.; Brachais, C.; Kurek, M.; Galić, K.; Debeaufort, F. Bioactive Antioxidant Coatings for Poly(Lactic Acid) Packaging Films: Polyphenols Affect Coating Structure and Their Release in a Food Simulant. *J. Sci. Food Agric.* **2023**, *103*, 1115–1126. [CrossRef] [PubMed]
75. Qamar, S.A.; Comune, L.; Diglio, C.; Petraglia, A.; Rubino, M.; Piccolella, S.; Pacifico, S. Biobased Films from 'Annurca' Apple Processing Waste: Isolated Cellulose and Polyphenols Combined for Functional Materials Development. *Food Res. Int.* **2026**, *223*, 117838. [CrossRef]
76. Maciel, F.S.; Assis, R.Q.; Rios, A.d.O.; Pertuzatti, P.B. Açaí Powder-Enriched Biodegradable Starch Films: Characterization, Release in Food Simulants and Protective Effect in Photodegradation System. *Int. J. Biol. Macromol.* **2025**, *308*, 142420. [CrossRef] [PubMed]